J. Membrane Biol. 73, 217–226 (1983)

The Journal of
Membrane Biology

Ion Conductances of the Surface and Transverse Tubular Membranes of Skeletal Muscle

L.E. Moore and T.D. Tsai*
Department of Physiology and Biophysics, University of Texas Medical Branch, Galveston, Texas 77550

Summary. A combination voltage clamp and admittance analysis of single skeletal muscle fibers showed that moderate depolarizations activated a steady-state negative sodium conductance in both the surface and transverse tubular membranes. The density of the voltage-dependent channels was similar for the surface and tubular conductances. The relaxation times associated with the negative conductance were in the millisecond range and markedly potential dependent. The negative tubular conductance has the consequence of increasing the apparent steady-state radial space constant to large values. This occurs because the positive conductance is counterbalanced by the maintained inward-going sodium current. The enhancement of the space constant by a negative conductance provides a means for the nearly simultaneous activation of excitation-contraction coupling.

Key Words transverse tubules · admittance · impedance · excitation-contraction coupling · ion conductances · muscle

Introduction

The analysis of the electrical properties of skeletal muscles has been done with many different techniques, ranging from resting potential (Hodgkin & Horowicz, 1960) and voltage-clamp experiments (Adrian, Chandler & Hodgkin, 1969) to inferences about radial propagation of action potentials based on myofibrillar contractions (Adrian, Costantin & Peachey, 1969; Gonzallez-Serratos, 1971; Costantin, 1975). The unique feature of excitability in skeletal muscle, compared to the more exhaustively investigated axonal membranes, is the presence of the transverse tubular membrane system which serves the key function of excitation-contraction coupling. Falk and Fatt (1964), using small signal alternating current methods, were among the first to clearly point out the consequences of the tubular membrane in an equivalent circuit analysis in which the apparent high capacitance of muscle was shown to be accounted for by the infolding of the surface membrane to form the transverse tubular system. The nature of the electrical continuity between the surface and interior of the fiber has been investigated by a variety of optical and electrical methods (Bastian & Nakajima, 1974; Bezanilla & Horowicz, 1975; Oetliker, Baylor & Chandler, 1975; Vergara, Bezanilla & Salzberg, 1978; Nakajima & Gilai, 1980), leading to the general hypothesis that the transverse tubular membrane is excitable and normally propagates an action potential from the surface membrane to the interior of the fiber (Costantin, 1975; Nakajima & Bastian, 1976).

The purpose of this paper is to measure the voltage-dependent properties of these two membrane regions using a combination of the voltage-clamp and frequency domain white noise techniques (Fishman, Poussart, Moore & Siebenga, 1977). The previous voltage-clamp analyses of muscle have generally assumed either that the contribution of currents from an uncontrolled tubular membrane is relatively small compared to the total current or that the radial space constant is sufficiently large that the tubules are essentially equipotential with the surface membrane (Adrian, Chandler & Hodgkin, 1970; Moore, 1972; Hille & Campbell, 1976). The validity of these assumptions is critical for the voltage-clamp analysis of skeletal muscle; otherwise uncontrolled currents distort the measured responses and very likely invalidate the kinetic analysis.

The white noise admittance technique allows an estimation of the tubular properties and thus provides a means to analyze both the surface and tubular membrane parameters at different steady-state membrane potentials (Moore, 1981). These experiments show that both the surface and tubular membranes have a steady-state negative conductance which is sensitive to tetrodotoxin. The

* Visiting Scientist from Shanghai Institute of Physiology, Academia Sinica, Shanghai, China.

negative conductance of the transverse-tubular system counterbalances the relatively low positive conductance of the tubules which has the effect of increasing the apparent tubular membrane resistance. These results lead to the conclusion that for moderate depolarizations the steady-state radial space constant increases to large values thus providing an efficient mechanism for the rapid propagation of the surface potential throughout the branched tubular system. The increase of the radial space constant by a negative conductance enhances the normal radial propagation of an action potential to allow nearly simultaneous activation of excitation-contraction mechanisms throughout the fiber. This analysis further shows that the density of the voltage-dependent channels is similar for the surface and tubular membranes. The relaxation time constant for the negative conductance was potential dependent with values in the millisecond range. A positive conductance was observed at moderate to large depolarizations having a time constant an order of magnitude larger than observed for the negative conductance.

Materials and Methods

Voltage-Clamp System

The vaseline gapped voltage clamp for single skeletal muscle fibers, developed by Frankenhaeuser, Lindley and Smith (1966), Moore (1972) and Hille and Campbell (1976) was redesigned to provide significantly increased stability and frequency response. The current was determined differentially by measuring the potential across a 10 kΩ resistor in series with the output of the clamp amplifier. The method relies on a Vaseline coat of the fiber in the reference pool, which simulates a myelin sheath, thus preventing current flow through the membrane in this pool. The additional seal appears preferable since it effectively prevents a current path through the membrane to ground from within the fiber. Without the seal this pathway is in the feedback loop of the potentiometric amplifier, and could lead to distortion in the measurement of the membrane potential.

The voltage-clamp system consists of four independent wideband amplifier sections each of which has greater than 10 MHz bandwidth. When a passive R/C model (resistance and capacitance in parallel) is used, there was no need to provide a compensation for feedback loop stabilization because each section has a very wide bandwidth. The phase shifts that occur in these sections are very small; therefore, the R/C time constant dominates in the decline of the open loop gain with increasing frequency. However, when an actual membrane is in the loop, the phase shift in the membrane often approaches 180° at very high frequencies, and oscillations may occur at several megahertz. The system was stabilized by inserting a capacitor in the clamp amplifier to provide the desired roll-off. A 6 dB/octave low pass filter at 10 kHz ensured stability for most muscle membranes. It should be noted that even with such filtering the feedback loop has a gain of 1,000 at 100 kHz.

Single fibers were carefully dissected from the semitendinosus muscle of the bullfrog *Rana catesbeiana* and mounted in the Vaseline gap chamber containing potassium phosphate solution (67 mM K_2PO_4, 33 mM KH_2PO_4) buffered at pH 7.2. The fibers were mounted in a sodium-free solution to prevent excitability under the seals. After the seals were firmly applied, the solution in the recording pool was changed to normal Ringer's solution. The fibers were maintained at a slightly stretched length and were cut at each end, 300 to 400 μm from the seal edge. The holding potential was set at −90 mV.

The external solutions were as follows: normal Ringer's (mM) 120 NaCl, 2.5 KCl, 2.0 $CaCl_2$, 2.5 $NaHCO_3$. The pH of all solutions was adjusted to 7.2. All measurements were made at 12 °C.

Admittance Measurement

A combination of a "white noise" control signal with the voltage-clamp technique was used to make an admittance analysis at different membrane potentials. The step voltage-clamp method has proven itself as a powerful tool in the analysis of highly nonlinear excitable membranes. It is bascially a measurement of a transient response to a step perturbation. On the other hand, admittance measurements are usually made under steady-state conditions, which in the past required long periods of time, because responses to single sine waves had to be measured. The utility of "white noise" methods is that the preparation can be stimulated at all frequencies within the time period of the lowest frequency of interest and a response measured simultaneously. This procedure reduces the measurement time to an arbitrarily small value dependent only on the lowest frequency analyzed. In these experiments, a 400-line frequency spectrum from 2.5 Hz to 1 kHz required 400 ms of data.

The combination method requires that the response of the membrane to a large voltage-clamp step reach a quasi-steady state and then the small signal admittance measurement can be done. Thus, for each steady-state condition, defined by a mean membrane potential, a small-signal white noise voltage perturbation (~1 mV rms) superimposed on the step potential was applied to the clamp and the admittance measured. Linearity was assured by doubling the perturbation and observing the same transfer function (Moore, Fishman & Poussart, 1980). The step preceded the analysis period by 200 ms and thus had a total duration of 600 ms. For large step depolarizations, such an admittance measurement is subject to the effects of tubular depletion or accumulation typical of any voltage-clamp measurement. Apart from changes in the driving forces these phenomena should not affect admittance above 1 Hz (Barry, 1977).

The implementation of the "white noise" admittance (Poussart, Moore & Fishman, 1977) was done on an LSI-11/I computer system. A "white noise" stimulus was computed by summing 400 sine waves with random phases and amplitudes of unity for each frequency increment (1 to 400). A total of 1,024 time values were computed and sequentially output with a crystal clock via a 12-bit digital to analog (D/A) converter. The response of the preparation was digitized with a 12-bit analog to digital converter (A/D). The same clock signal was used to synchronize the D/A and A/D conversion. In order to ensure a steady-state response to white noise, the 1024 point sequence was applied twice for a total of 2048 clock pulses with a total duration of 800 ms. The pulse was applied at the midpoint of the first 1024 point sequence and the data was sampled during the second 1024 point sequence with the A/D converter. Before the A/D conversion, the analog response was low-pass filtered with a 96 db/octave roll-off Butterworth filter (Rockland 852). The stimulus was also low-pass filtered with a six-pole active filter (Frequency Devices). All low-pass filters were set at 1 kHz. In order to remove the direct current the

output of the current amplifier of the voltage-clamp system was high-pass filtered at 2 Hz with a single pole R/C filter.

In order to remove any filter responses or other coherent trends in the data a procedure called coherence elimination was used. In this procedure two identical step-clamp pulses were given as voltage-clamp commands; however, the small noise signal was inverted during the second pulse. The responses of the two perturbations were subtracted, thus eliminating coherent signals and adding the responses to the noise stimulus.

An improvement in the dynamic range of measurement was made by modifying the white noise stimulus to partially match the inverse of the response. A Lorentzian function with the corner frequency at the 67th line of the 400-line spectrum was used to change the sine wave amplitudes. The response of the fiber to this source was relatively flat providing a much improved dynamic range.

The system was calibrated by measuring the transfer function of a model system with a membrane resistance of 6 MΩ. The data for all fibers were scaled to give an admittance per cm^2 by using an estimated surface area of $3.4 \times 10^{-4} cm^2$. More than sixty fibers were investigated showing a range in the estimated surface membrane capacitance of 0.7 to 1.3 μF per cm^2.

The procedure for measuring the transfer function is as follows: (1) determine the complex spectrum of the source, filters and measurement system; (2) store the spectrum in a reference buffer; (3) measure the response of the preparation; (4) compute the ratio of the magnitude of the response and the reference; and (5) subtract the phases of the response and reference.

The magnitude and phase of the admittance are displayed and stored in a data file for subsequent plotting and analysis. All complex spectra are computed using a Fast Fourier Analysis (FFT) routine (Bendat & Piersol, 1971). The results of the FFT have been compared with hardwired spectrum analyzers and expected responses from known sources.

Analysis

The data were collected and stored as complex admittances with 400 real and 400 imaginary numerical values. The excitable membrane element was modeled as a collection of three parallel paths consisting of a membrane capacitance, a frequency independent conductance, and frequency dependent conductances (Chandler, Fitz Hugh & Cole, 1962). The formulation of the model is shown in Eq. (1):

$$Y_s = j2\pi f C_m + G_m + \sum_i \frac{G_i}{1 + j2\pi f \tau_i} \quad (1)$$

where Y_s is the complex surface membrane admittance, G_m is the frequency independent steady-state conductance, C_m is the membrane capacitance, G_i is a frequency dependent conductance, τ_i is the time constant associated with G_i, j is $\sqrt{-1}$, and f is the frequency in hertz. This formulation is perfectly general and is completely equivalent to the linearized Hodgkin-Huxley (HH) formalism (Hodgkin & Huxley, 1952) where the conductances are complicated functions of steady-state parameters (Mauro, Conti, Dodge & Schor, 1970). The time constants in the two formulations are identical. In the HH formalism a negative G_i would reflect the activation or m process of the sodium system and positive G_i's would be equivalent to either the inactivation h process of the negative sodium conductance or the activation n process of the potassium system.

The total admittance Y is the sum of the surface Y_s and tubular Y_t admittance. The tubular admitance was evaluated by the numerical model described by Peachy and Adrian (1973) consisting of 16 shells each of which was scaled according to their surface area by the factor $k^2-(k-1)^2$, where k is the shell number. Each shell contained the parallel paths of Eq. (1). The tubular admittance was determined iteratively by first computing the innermost shell admittance and then subsequently adding the next shells individually. Initially estimates were given each parameter in the model and the real and imaginary components were computed and compared with the data points for calculation of a chi square value. The chi square was minimized by two curve-fitting routines, the grid and chi square gradient search methods (Bevington, 1969). All of the curve fitting was done on a PDP 11/70 with complex numbers using a slight modification of the Fortran subroutines of Bevington (1969).

Results

Conventional step-voltage clamp measurements were done to assure the presence of transient inward and steady-state outward currents. All measurements on properly mounted, well-dissected fibers showed uncontrolled, presumably tubular currents (Mandrino, 1977). Fibers which were poorly dissected, mounted in a contracted or shortened state, or inactivated, generally provided membrane currents which appeared to be graded and properly controlled. Comparison of the admittance functions, in Fig. 1, of these two types of fibers suggests that the transverse tubular system is less accessible in the latter. The curves labeled $F1$ are magnitude and phase functions from a carefully dissected fiber. Note the initial peak in the phase around 30 Hz and a slight inflection in the magnitude at somewhat higher frequencies. The smooth curve drawn through the data is the best least-square fit of the surface and tubular membrane model discussed above. The theoretical curves labeled R/C are from the same model without the transverse tubular system. These curves show the admittance of the passive surface membrane containing only a resistance and capacitance in parallel. The curves labeled $F2$ are from the second type of fiber which does not show a pronounced hump in the phase. Note that the magnitude and phase functions of this fiber are intermediate between the normal fiber with an intact T-system, and a simple R/C equivalent circuit with no T-system. This suggests that certain types of procedures may partially disrupt the tubules and thereby appear to allow an adequate voltage clamp on the surface membrane. The experiments reported here are only from fibers which clearly demonstrate an intact transverse tubular system.

The superimposed curves of Fig. 2 show the general behavior of the total admittance for a fiber bathed in normal Ringer's solution. The data points and model fits are expressed as magnitude and phase functions versus frequency. The curves

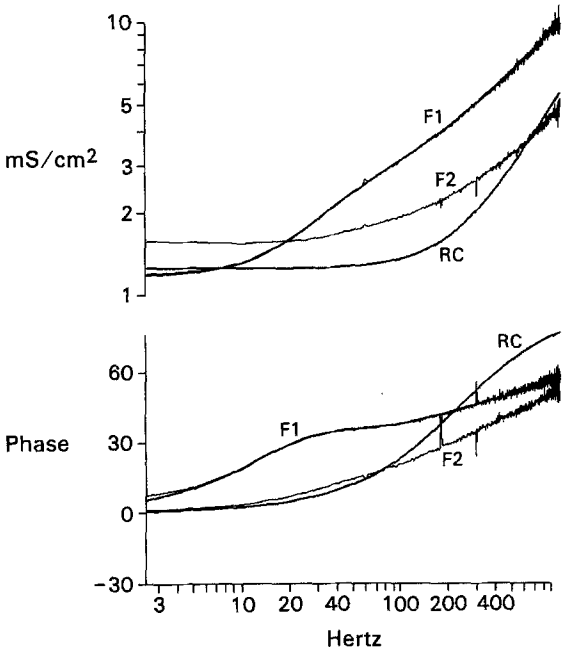

Fig. 1. Magnitude and phase functions of resting muscle fibers. Four complex admittance functions are shown. Each function consists of a magnitude and a phase versus frequency. The upper portion of the Figure is the magnitude in millisiemens per cm^2 versus frequency in hertz. The lower portion is the phase in degrees. The magnitude and phase plots labeled *F*1 are data from a fiber in good condition. A model fit based on Eq. (1) with a 16 shell transverse tubular system is superimposed on this data. The model without the transverse tubular system is superimposed on this data. The model without the transverse tubular system is shown as *R*/*C*. The values of the surface resistance and capacitance are identical to the model of *F*1. Note that the T-system influences the admittance function over a wide frequency range. The plots labeled *F*2 are from a contracted muscle fiber which produced good voltage-clamp currents. The admittance of the fiber is not a simple *R*/*C* function; however, the T-system is considerably different from the normal fiber of *F*1. In this and subsequent Figures the model fits are smooth lines superimposed on the connected data points

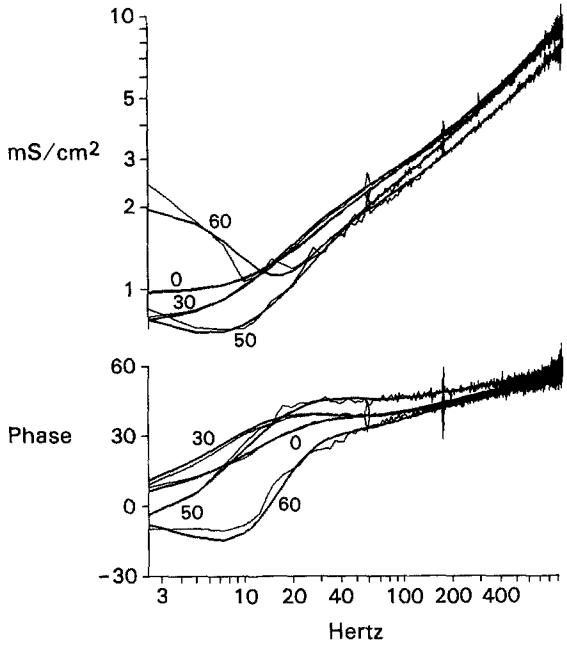

Fig. 2. Complex admittance in normal Ringer's solution. Data and model fits are superimposed for admittances measured at the resting potential of −90 mV, labeled O, and depolarizations of 30, 50 and 60 mV

labeled O illustrate the typical behavior of the resting surface and tubular membranes similar to that shown in Fig. 1.

The step depolarizations used in Fig. 2 show the principle phenomena elicited by an activation of the voltage-dependent conductances. The 30-mV depolarization shows three prominent features: (1) a decrease in the low frequency magnitude, (2) an increase in the initial phase peak at ~20 Hz, and (3) an enhancement of the inflection of the magnitude seen at ≈50 Hz. The finding of a decrease in the low frequency admittance magnitude is opposite to the generally expected conductance increases seen with depolarizations. The admittance is a measure of the frequency dependence of a slope conductance and can therefore be positive or negative. These phenomena are adequately described by negative conductances in the surface and tubular membranes. Attempts to model the data with decreasing positive conductances were unsuccessful.

The 50-mV depolarization shows the additional feature of a slight minimum in the magnitude (anti-resonance) around 10 Hz accompanied by shift to higher frequencies of the transition region of the phase function. The transition region begins at small or negative values and shifts to positive values within a few Hertz. The shift and enhancement of the phase function along with the anti-resonance of the magnitude are indicative of ionic conductance relaxations (Fishman, Poussart & Moore, 1979; Mathias, Ebihara, Lieberman & Johnson, 1981). In addition, the 50-mV depolarization led to a decrease in the magnitude over a wide frequency range, consistent with the activation of a high frequency negative sodium conductance.

Finally, the 60-mV depolarization shows a pronounced anti-resonance and a negative phase which shows a sharp transition to positive values at ~20 Hz. The frequency location of the anti-resonance minimum and the phase transition are shifted to higher frequencies the greater the depolarization, indicative of shorter relaxation times seen at these potentials.

The admittance functions of Fig. 2 are com-

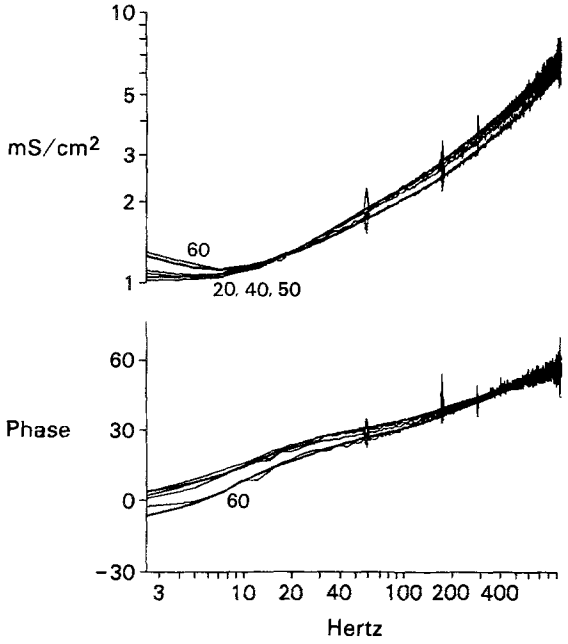

Fig. 3. Complex admittance in 10^{-6} mM TTX Ringer's solution. The magnitude and phase plots for the three depolarizations of 20, 40 and 50 mV are virtually identical. The plots for a 60-mV depolarization show slight anti-resonances in the data and fitted curves

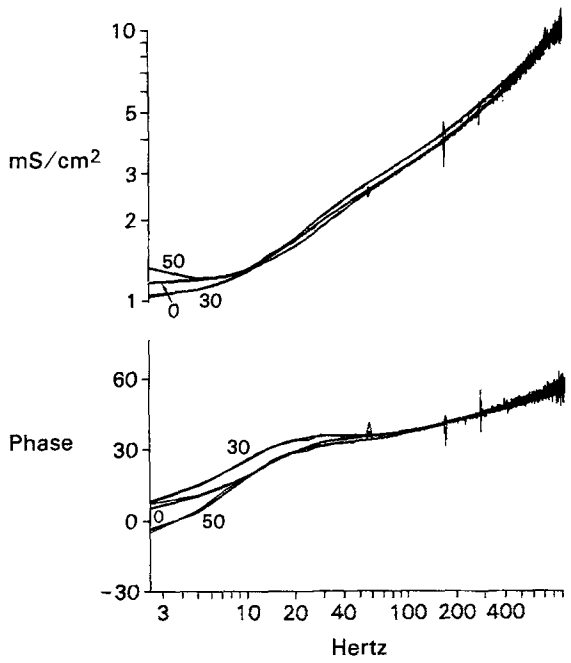

Fig. 4. Admittance of activated tubular membrane. These measuements were made soon after the TTX blockage of the surface sodium conductances. The three superimposed functions and model fits are shown for 0-, 30- and 50-mV depolarizations

posed of active surface and tubular conductances which are not easily separated. The sensitivity of these phenomena to 10^{-6} M tetrodotoxin (TTX) is shown in Fig. 3. The admittances for 20-, 40- and 50-mV depolarizations are essentially identical; however, the 60-mV depolarization shows a slight anti-resonance probably related to the potassium conductance system. Thus, depolarizations up to 50 mV induce mainly TTX sensitive admittances which can be identified with a negative steady-state sodium ion conductance system. The steady-state potassium admittance was not observed for membrane potentials less negative than -40 mV. The lack of a significant steady-state potassium conductance at -40 mV was confirmed by voltage-clamp currents observed during the admittance measurement interval which began 200 ms after the step change in membrane potential. This result is consistent with the earlier observations (Adrian et al., 1970; Moore, 1972) which generally show the late ionic currents beginning to activate at -40 mV (≈ 50 mV depolarization). This is also the potential at which the peak inward current appears. Although the long voltage-clamp pulses partially inactivate the sodium conductance, the large driving force for the sodium current maximizes the negative slope conductance in the potential range investigated.

The method used to separate the surface and tubular conductance relied on the diffusion time for TTX to equilibrate with the T-tubule sodium conductance sites. In the experiment of Fig. 4 the normal Ringer's external solution was changed to one containing 10^{-6} M TTX within 10 s. The admittance measurements were made within 1 min approximately 30 s after the solution change. A separate experiment confirmed that the action potential was completely blocked within 30 s. Since the equilibration time for the T-tubule is 5 min or longer (Bastian & Nakajima, 1974; Almers & Levinson, 1975), these measurements were made with TTX principally blocking the surface membrane. Under these conditions a step depolarization mainly activated a negative tubular sodium conductance. In Fig. 4, the admittance at a 30-mV depolarization compared to that observed at the resting potential shows a decrease in magnitude at low frequencies. This result is qualitatively similar to that observed without TTX in Fig. 2; however, the changes with potential are significantly less. This finding is consistent with the hypothesis that a depolarization applied immediately after

blockage of the surface sites by TTX will preferentially activate the tubular sodium conductance. The model used for curve fits of the admittance at the depolarizations shown in Fig. 4 were made with a negative conductance only in the tubules.

The 50-mV depolarization of Fig. 4 shows an anti-resonance in the magnitude of the admittance which is most likely due to the sodium inactivation process in the tubules since TTX at long times and moderate depolarizations blocks the anti-resonance of both the surface and tubular membranes. Furthermore, unpublished experiments in which the potassium conductance was blocked by 50 mM tetraethylamonium-chloride (TEA) and 2.5 mM RbCl showed an anti-resonance for a 50-mV depolarization. Therefore, the data of Fig. 4 were analyzed with a model containing positive and negative conductance relaxation components in the tubules. The two conductances are analogous to the activation m and inactivation h processes of the Hodgkin-Huxley formalism.

The analysis procedure consisted of initially estimating the passive membrane parameters where the G_i's of Eq. (1) are zero The parameters which could be uniquely determined were three: the surface membrane capacitance, the tubular membrane capacitance, and the resistance between the individual shells. The total tubular capacitance was estimated to be fivefold greater than the surface value, consistent with a larger membrane area in the T system than that estimated as surface area. The representative curve fit shown in Fig. 1 gave a surface membrane capacitance of 0.9 $\mu F/cm^2$ and a total tubular capacitance of 5.3 $\mu F/cm^2$. Although the passive surface and tubular membrane resistances cannot be uniquely determined it was possible to find a chi square minimum consistent with previous estimates of the radial space constant (Adrian et al., 1969). The curve fit of the resting fiber of Fig. 2 led to a passive radial space constant of three fiber diameters and a membrane resistance of 1 $k\Omega^2$ for both the surface and tubular membrane. These values are in good agreement with the previous analyses of the passive equivalent circuit of frog skeletal muscle (Falk & Fatt, 1964; Adrian et al., 1969; Schneider, 1970; Valdiosera, Clausen & Eisenberg, 1974*b*). For the frequency-range of the present measurements, the passive shell model has been shown to agree satisfactorily with the exact solution of the appropriate cable equations (Peachy & Adrian, 1973).

The analysis at depolarized potentials was done by using the previously determined resting values of the surface and tubular capacitances as constants in the model. The number of relaxation elements for the admittances was determined by the experimental condition. In Fig. 4 the active conductances were added to the tubules and a best fit obtained. A negative conductance was required to fit the data which had relaxation times of 2 and 1 ms for depolarizations of 30 and 50 mV, respectively. The anti-resonance seen for the 50-mV depolarization of Fig. 4 was fitted with an additional positive conductance having a time constant of 13 ms probably reflecting a slow sodium inactivation time constant. The observed decrease in the admittance could be due to three different conductance changes: (1) a decrease in the potassium conductance of the anomalous rectifier, (2) an activation of a negative calcium conductance, or (3) the activation of a negative sodium conductance. The anomalous rectifier is essentially turned off a these potential levels (Hodgkin & Horowicz, 1959). The calcium conductance is probably activated; however, the frequency range and membrane potential levels are not optimal for observing the calcium currents (Siri, Sanchez & Stefani, 1980; Almers & Palade, 1981). Since the major observed effects are TTX sensitive the most likely source of the admittance change is an activation of steady-state negative sodium conductance.

The admittance measurements of Fig. 2 and Fig. 5 in normal Ringer's solution can only be ana-

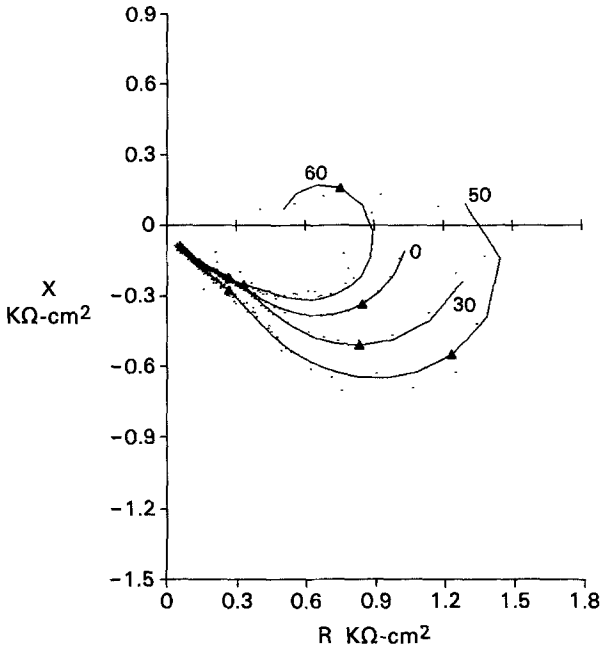

Fig. 5. Cole-Cole plot of complex impedance in normal Ringer's solution. The data and model fits are identical to Fig. 2. The triangles show the 10 and 100 hertz frequency points of the model. The numbers adjacent to each curve are the levels of depolarization from the resting level

lyzed if the tubular contribution is known. For a limited range of potentials this was done by fixing the parameters of the negative tubular conductance relaxation term (G_i and τ_i of Eq. 1) to the values determined in Fig. 4 and fitting the data with a voltage-dependent conductance in the surface membrane. For the 30-mV depolarization of Fig. 2 the fitted data for the two negative conductances had a surface time constant of 1 ms and a tubular value of 2 ms. The ratio of the two relaxation conductances (G_i) per unit area at zero frequency was essentially unity, consistent with the hypothesis that the channel density is similar for the surface and tubular membranes. The 50-mV depolarization of Fig. 2 was fitted with a positive surface conductance and a negative tubular conductance. The model fits the data well but cannot separate surface and tubular components. Since the analysis suggests a similarity for surface and tubular active conductances a different model was used in which the active conductances per unit area of both membrane systems were identical. This model fits the data extremely well and probably is the best estimate of the membrane properties for fibers in Ringer's solution. Using this model, time constants for the negative conductance were 6.9, 6.1, 2.7, 1.0 and 0.9 ms for 20-, 30-, 40-, 50-, and 60-mV depolarizations, respectively. The anti-resonance required an additional positive conductance for the 40-, 50-, and 60-mV depolarization which had time constants of 50, 52, and 22 ms, respectively.

The data of Fig. 2 were replotted in Fig. 5 as a Cole-Cole plot (Cole, 1941) in order to illustrate the effect of the ionic conuctances on the impedance function. The two triangles seen on each curve mark the frequencies, 10 and 100 Hz, reading from right to left. The curve labeled 0 is the resting impedance showing the characteristic double dispersion seen as the sum of two semi-circles (Cole, 1968). Note that the high frequency points extrapolate to the origin which indicates that there is no significant series resistance in the preparation.

The curves labeled *30* and *50* show the marked effect of activating a negative conductance which is seen here as an increasing low frequency reistance. The depolarizations of 50 and 60 mV have curves which cross the abscissa indicative of an anti-resonance and modeled by a positive conductance.

Discussion

The results of these experiments strongly support the hypothesis that the transverse tubular membrane of skeletal muscle has voltage-dependent conductances which are similar in kinetic behavior and density to those found on the surface membrane. This conclusion is consistent with the high density of TTX binding sites in the tubules (Jaimovich, Venosa, Shrager & Horowicz, 1976) and suggests a need to revise the action potential model of Adrian and Peachey (1973) which is based on extremely low channel densities.

The presence of a normal tubular system in skeletal muscle essentially prevents an adequate voltage-clamp analysis of large transient conductance changes. The apparent success of previous voltage-clamp measurements is probably the consequence of an altered tubular membrane system, which, under ideal conditions, could lead to a minimal distortion of the surface membrane currents. However, the results of Fig. 1 show that fibers which show graded currents may possess an altered tubular system which could produce uncontrolled responses. These conclusions are further supported by optical probe experiments which show uncontrolled tubular potentials despite an adequately clamped surface membrane (Heiny & Vergara, 1982).

The instability of the tubular system in the cut fibers was a generally observed phenomenon. Contracted or shortened fibers could remain excitable for hours but showed no prominent inflections in the phase function characteristic of a normal transverse tubular system. However, fibers which maintained a normal striation pattern invariably possessed a normal tubular system. Marked effects on the phase function also occurred in solutions of different osmolarity as would be expected by alterations in the tubular dimensions (*unpublished*). These observations, coupled with the well-known sensitivity of excitation-contraction coupling and the T-system to osmotic shocks (Fujino, Yamaguchi & Szuki, 1961; Eisenberg & Gage, 1969; Howell, 1969), lead to the general conclusion that an adequate voltage-clamp analysis requires a knowledge of the state of the T-system in order to evaluate the total current measured from the preparation.

The advantage of the admittance method is that it provides a good characterization of the T-system and a means to evaluate its properties. Although the measurements are restricted to linear responses it is possible to obtain time constants and steady-state conductances for both the surface and tubular membranes. The principle difficulties in this analysis are similar to those of the conventional voltage clamp, namely, the separation of ionic currents. In skeletal muscle the extra mem-

brane system requires procedures which differentially block the surface versus tubular membrane in order to uniquely characterize the conductances. Proper separation procedures are also critical for active versus passive membrane parameters. The detailed impedance experiments of Schneider (1970) and Valdiosera, Clausen and Eisenberg (1974*a–c*) have been interpreted on the basis of a passive surface and tubular membrane whose voltage-dependent conductances are insignificant under the conditions of the measurement. Unfortunately many of the reported impedance measurements have been made at somewhat depolarized membrane potentials where it can be expected that voltage-dependent ion conductance processes are present. The measurements of Schneider (1970) were done in 7.5 mM potassium ion concentration at an estimated membrane potential of −66 mV. Experiments discussed in this paper clearly indicate sodium conductance contributions to the admittance at these potentials. Also some of the measurements of Valdiosera, Clausen and Eisenberg (1974*c*) were done at depolarized potentials. For example, the perplexing results of a concomitant increase of the radial resistance and the tubular capacitance was based on data taken at a membrane potential of −65 mV. The presence of voltage-dependent ion conductances alters the equivalent circuit to a sufficient degree that passive and active (voltage-dependent) phenomena have similar circuits and may be indistinguishable in a given experiment.

The question of spatial control of the tubular potential can be considered from the analysis. At rest the radial space constant λ_t cannot be uniquely determined because of the equivalence at zero frequency of the surface or tubular resistances. However, for depolarizations which active a tubular conductance (*see* Fig. 4) an estimate of λ_t is possible.

The value of λ_t^2 was calculated from the ratio of the total transverse resistance within one tubular element and the resistance between the individual shells. Thus, λ_t^2 is equivalent to the transverse membrane resistance divided by the luminal resistance. The reciprocal of the membrane resistance was determined by algebraically adding the zero frequency conductances of a tubular element. Using curve fits with finite values for the tubular membrane resistance, the λ_t of resting or hyperpolarized fibers ranged from 2 to 10 fiber radii.

The value of λ_t for fibers at rest is consistent with earlier estimates; however, the steady-state negative conductance activated at moderate depolarizations led to an extremely large or slightly negative value for λ_t^2. Under these conditions the usual definition of λ_t breaks down and the boundary conditions for cable equations used to derive the space constant are incorrect. One difficulty in assessing the meaning of a negative λ_t^2 is that the effect is due to a counterbalancing of the total positive conductance by the negative conductance. At the null point this leads to an apparent infinite tubular membrane resistance. A similar result has been observed in the squid axon when the positive potassium conductance is blocked by internal cesium ions (Fishman et al., 1979). The discontinuity at the null point can be approached from either a diminishing net positive or negative conductance. Whether or not the tubular conductance in fact has a net negative steady-state value is model dependent; however, the analysis clearly indicates that the activation of the negative tubular conductance has the effect of greatly increasing the apparent tubular membrane resistance. This conclusion means that for 600-ms depolarizing pulses the tubular membrane was essentially more equipotential with the surface than would be predicted from the resting radial space constant.

The negative tubular conductance thus enhances the propagation of any potential waveform by increasing the radial space constant despite the fact that the absolute value of the membrane resistance decreases. This mechanism enhances the propagation of action potentials and allows for a nearly simultaneous activation of the entire branched tubular structure.The negative tubular conductance also improves the voltage clamp which may account for the reason graded currents are often observed under conditions in which potential control of the tubules would generally not be possible.

The negative conductance due to tubular calcium currents would further enhance the above effects. In general, the steady-state negative conductance enhancement of the space constant of narrow tubes or processes probably plays an important role in the propagation of potentials in a variety of branched excitable structures. The presence of noninactivating sodium and calcium conductances in dendritic membranes provides a way to propagate synaptic potentials to the cell body even if the density of channels is insufficient to generate an action potential. In addition, this mechanism could provide a method for incremental propagation in small processes.

The enhancement of the space constant by a negative conductance is probably unique to small structures which have large longitudinal resistances that tend to decrease the value of the space con-

stant. Large axons have correspondingly lower longitudinal resistances and generally possess a significant potassium conductance which cannot be overcome in the steady state by a negative sodium conductance. However, at rest the squid axon does possess a steady-state negative sodium conductance which can be observed by blocking the conductance with TTX (Fishman et al., 1979).

In skeletal muscle the resting potential is sufficiently high that the negative conductances are extremely low. In nerve cells the resting potental is 20 to 30 mV more depolarized which may provide a continuously active sodium or calcium conductance. In cells with a low positive conductance the negative conductance provides a functionally high membrane resistance somewhat analogous to myelin, enhancing the propagation of all types of potentials.

We wish to thank Dr. T. Iwazumi for designing and constructing the voltage clamp used in these experiments. This work was supported in part by N.I.H. Grant NS-13520.

References

Adrian, R.H., Chandler, W.K., Hodgkin, A.L. 1969. The kinetics of mechanical activation in frog muscle. *J. Physiol (London)* **204**:207–230

Adrian, R.H., Chandler, W.K., Hodgkin, A.L. 1970. Voltage clamp experiments in striated muscle fibers. *J. Physiol. (London)* **208**:607–644

Adrian, R.H., Constantin, L.L., Peachey, L.D. 1969. Radial spread of contraction in frog muscle fibres. *J. Physiol. (London)* **204**:231–257

Adrian, R.H., Peachey, L.D. 1973. Reconstruction of the action potential of frog sartorius muscle. *J. Physiol (London)* **235**:103–131

Almers, W., Levinson, S.R. 1975. Tetrodotoxin binding to normal depolarized frog muscle and the conductance of a single sodium channel. *J. Physiol. (London)* **247**:483–509

Almers, W., Palade, P.T. 1981. Slow calcium and potassium currents across frog muscle membrane measurements with the vaseline-gap voltage clamp technique. *J. Physiol. (London)* **312**:159–176

Barry, P.H. 1977. Transport number effects in the transverse tubular system and their implications for low frequency impedance measurement of capacitance of skeletal muscle fibers. *J. Membrane Biol.* **34**:383–408

Bastian, J., Nakajima, S. 1974. Action potential in the transverse tubules and its role in the activation of skeletal muscle. *J. Gen. Physiol.* **63**:257–278

Bendat, J.S., Piersol A.G. 1971. Random Data: Analysis and Measurement Procedures. Wiley-Interscience, New York

Bevington, P.R. 1969. Data Reduction and Error Analysis for the Physical Sciences. McGraw-Hill, New York

Bezanilla, F., Horowicz, P. 1975. Fluorescence intensity changes associated with contractile activation in frog muscle stained with Nile Blue A. *J. Physiol. (London)* **246**:709–735

Chandler, W.K., FitzHugh, R., Cole, K.S. 1962. Theoretical stability properties of a space-clamped axon. *Biophys. J.* **2**:105–128

Cole, K.S. 1941. Rectification and inductance in the squid giant axon. *J. Gen. Physiol.* **25**:29

Cole, K.S. 1968. Membranes, Ions and Impulses. 1972 revised edition. University of California Press, Berkeley

Costantin, L.L. 1975. Contractile activation in skeletal muscle. *Prog. Biophys. Mol. Biol.* **29**:197–224

Eisenberg, R.S., Gage, P.W. 1969. Ionic conductances of the surface and transverse tubular membranes of frog sartorius fibers. *J. Gen. Physiol.* **53**:279–297

Falk, G., Fatt, P. 1964. Linear electrical properties of striated muscle fibers observed with intracellular electrodes. *Proc. R. Soc. London B* **160**:69–123

Fishman, H.M., Poussart, D., Moore, L.E. 1979. Complex admittance of Na^+ conduction in squid axon. *J. Membrane Biol.* **50**:43–63

Fishman, H.M., Poussart, D.J.M., Moore, L.E., Siebenga, E. 1977. K^+ conduction description from the low frequency impedance and admittance of squid axon. *J. Membrane Biol.* **32**:255–290

Frankenhaeuser, B., Lindley, B.D., Smith, R.S. 1966. Potentiometric measurement of membrane action potentials in frog muscle fibers. *J. Physiol (London)* **183**:152–166

Fujino, M., Yamaguchi, M., Suzuki, K. 1961. Glycerol effect and the mechanism linking excitation of the plasma membrane with contraction. *Nature (London)* **192**:1159–1161

Gonzalez-Serratos, H. 1971. Inward spread of activation in vertebrate muscle fibres. *J. Physiol (London)* **212**:777–799

Heiny, J.A., Vergara J. 1982. Optical recordings of surface and T-system transmembrane potentials in skeletal muscle. *Biophys. J.* **37**:24a

Hille, B., Campbell, D.T. 1976. An improved vaseline gap voltage clamp for skeletal muscle fibers. *J. Gen. Physiol.* **67**:265–293

Hodgkin, A.L., Horowicz, P. 1959. The influence of potassium and chloride ions on the membrane potential of single muscle fibres. *J. Physiol. (London)* **148**:127–160

Hodgkin, A.L., Horowicz, P. 1960. The effect of sudden changes in ionic concentrations on the membrane potential of single muscle fibres. *J. Physiol. (London)* **153**:370–385

Hodgkin, A.L., Huxley, A.F. 1952. A quantitative description of membrane current and its application to conduction and excitation in nerve. *J. Physiol. (London)* **117**:500–544

Howell, J.N. 1969. A lesion of the transverse tubules of skeletal muscle. *J. Physiol. (London)* **210**:515

Jaimovich, E., Venosa, R.A., Shrager, P., Horowicz, P. 1976. Density and distributions of tetrodotoxin receptors in normal and detubulated frog sartorius muscle. *J. Gen. Physiol.* **67**:399–416

Mandrino, M. 1977. Voltage-clamp experiments on frog single skeletal muscle fibres; Evidence for a tubular sodium current. *J. Physiol. (London)* **269**:605–625

Mathias, R.T., Ebihara, L., Lieberman, M., Johnson, E.A. 1981. Linear electrical properties of passive and active currents in spherical heart cell clusters. *Biophys. J.* **36**:221–242

Mauro, A., Conti, F., Dodge, F., Schor, R. 1970. Subthreshold behavior and phenomenological impedance of the squid giant axon. *J. Gen. Physiol.* **55**:497–523

Moore, L.E. 1972. Voltage clamp experiments on single muscle fibers of *Rana pipiens*. *J. Gen. Physiol.* **60**:1–19

Moore, L.E. 1981. White noise analysis of voltage dependent ion conduction in voltage clamped skeletal muscle fibers. *Biophys. J.* **33**:285a

Moore, L.E., Fishman, H.M. Poussart D.J.M. 1980. Small-signal analysis of K^+ conduction in squid axons. *J. Membrane Biol.* **54**:157–164

Nakajima, S., Bastian, J. 1976. Membrane properties of the transverse tubular system of amphibian skeletal muscle. *In:*

Electrobiology of Nerve, Synapse, and Muscle. J.P. Reuben, D.P. Purpura, M.V.L. Bennett and E.R. Kandel, editors. pp. 243–267. Raven Press, New York

Nakajima, S., Gilai, A. 1980. Radial propagation of muscle action potential along the tubular system examined by potential-sensitive dyes. *J. Gen. Physiol.* **76**:751–762

Oetliker, H., Baylor, S.M., Chandler, W.K. 1975. Simultaneous changes in fluorescence and optical retardation in single muscle fibres during activity. *Nature (London)* **257**:693–696

Peachey, L.D., Adrian, R.H. 1973. Electrical properties of the transverse tubular system. *In:* The Structure and Function of Muscle. G.H. Bourne, editor. Vol. III., pp. 1–30. Academic Press, New York

Poussart, D., Moore, L.E., Fishman, H. 1977. Ion movements and kinetics in squid axon. I. Complex admittance. *Ann. N.Y. Acad. Sci.* **303**:355–379

Schneider, M. 1970. Linear electrical properties of the transverse tubules and surface membrane of skeletal muscle fibers. *J. Gen. Physiol.* **56**:640–671

Siri, L.N., Sanchez, J.A., Stefani, E. 1980. Effect of glycerol treatment on the calcium current of frog skeletal muscle. *J. Physiol. (London)* **305**:87–96

Validosera, R., Clausen, C., Eisenberg, R.S. 1974*a*. Measurement of the impedance of frog skeletal muscle fibers. *Biophys. J.* **14**:295–315

Valdiosera, R., Clausen, C., Eisenberg, R.S. 1974*b*. Circuit properties of the passive electrical properties of frog skeletal muscle fibers. *J. Gen. Physiol.* **63**:432–459

Valdiosera, R., Clausen, C., Eisenberg, R.S. 1974*c*. Impedance of frog skeletal muscle fibers in various solutions. *J. Gen. Physiol.* **63**:460–491

Vergara, J., Bezanilla, F., Salzberg, B. 1978. Nile blue fluorescence signals from cut muscle fibers under voltage or current clamp conditions. *J. Gen. Physiol.* **72**:775–800

Received 16 July 1982; revised 24 November 1982